eXPRESS Polymer Letters Vol.1, No.12 (2007) 837–845
Available online at www.expresspolymlett.com
DOI: 10.3144/expresspolymlett.2007.116

Relaxation phenomena in rubber/layered silicate nanocomposites

G. C. Psarras[1], K. G. Gatos[2], P. K. Karahaliou[1,3], S. N. Georga[3], C. A. Krontiras[3], J. Karger-Kocsis[2]*

[1]Department of Materials Science, School of Natural Sciences, University of Patras, Patras 26504, Greece
[2]Institute for Composite Materials, Kaiserslautern University of Technology, Erwin Schrödinger Str., Kaiserslautern, D-67663, Germany
[3]Department of Physics, School of Natural Sciences, University of Patras, Patras 26504, Greece

Received 27 July 2007; accepted in revised form 10 November 2007

Abstract. Broadband Dielectric Spectroscopy (BDS) is employed in order to investigate relaxation phenomena occurring in natural rubber (NR), polyurethane rubber (PUR) and PUR/NR blend based nanocomposites, reinforced by 10 parts per hundred (phr) Layered Silicates (LS). Nanocomposites and matrices were examined under identical conditions in a wide frequency (10^{-1} to 10^6 Hz) and temperature (–100 to 50°C) range. Experimental data are analyzed in terms of electric modulus formalism. The recorded relaxation phenomena include contributions from both the polymer matrices and the nanofiller. Natural rubber is a non-polar material and its performance is only slightly affected by the presence of layered silicates. Polyurethane rubber exhibits four distinct relaxation processes attributed, with ascending relaxation rate, to Interfacial Polarization (IP), glass/rubber transition (α-mode), local motions of polar side groups and small segments of the polymer chain (β, γ-mode). The same processes have been detected in all systems containing PUR. IP is present in all nanocomposites being the slowest recorded process. Finally, pronounced interfacial relaxation phenomena, occurring in the PUR+10 phr LS spectra, are attributed to nanoscale effects of intercalation and exfoliation.

Keywords: *polymer composites, nanocomposites, dielectric spectroscopy, relaxations, rubber*

1. Introduction

The impact of nanomaterials and/or nanostructured materials is well known and well appreciated [1–4], mostly due to their potential applications based on their thermo-mechanical performance, flame resistance, electrical properties etc. Polymer matrix nanocomposites can be prepared by dispersing a small amount of nanometer size filler within the host medium. Rubber/Layered Silicate (LS) nanocomposites are increasingly attracting scientific and technological attention, because of the high reinforcing efficiency of the LS, even at very low loading. Polymer matrix/LS nanocomposites exhibit three different configurations: (a) microphase separated composites, where polymer matrix and layered silicates remain immiscible, (b) intercalated structures, where polymer molecules are inserted between the silicate layers, and (c) exfoliated structures, where individual silicate layers are dispersed in the polymer matrix.

Polymer matrix nanocomposites are expected to be useful in replacing conventional insulating materials providing tailored performance, by simply controlling the type and the concentration of nanoinclusions [5–8]. 'Nanodielectrics' is a rather new term associating dielectrics with nanotechnology [9]. Nanoinclusions could be able to serve as inherent nanocapacitors. Charging and discharging

*Corresponding author, e-mail: G.C.Psarras@upatras.gr

under control the embedded in a matrix nanocapacitors, defines an energy storing procedure at the nanoscale level introducing a new type of nanodevices.

Broadband Dielectric Spectroscopy (BDS) is a powerful tool for the investigation of molecular mobility, phase transitions, conductivity mechanisms and interfacial effects in polymers and complex systems [10]. In the present study, natural rubber, polyurethane rubber and natural/polyurethane blend based nanocomposites were prepared by adding a pristine synthetic layered silicate (sodium fluorohectorite) in 10 parts per hundred parts rubber, following the latex compounding route. The dielectric properties, of the produced nanocomposites, were examined by means of BDS at temperatures varying from –100 to 50°C.

2. Experimental

A synthetic sodium fluorohectorite (Somasif ME-100) of Co-op Chemicals (Tokyo, Japan) was used as LS. This LS has an intergallery distance of 0.95 nm and exhibits a very high aspect ratio, viz. >1000. Sulfur prevulcanized NR latex was procured from the Rubber Research Institute of India (Kottayam, Kerala, India). PUR latex (Impranil DLP-R) containing ca. 50% polyester-based polyurethane was supplied by Bayer AG (Leverkusen, Germany). The produced nanocomposites were all containing the same amount of nanofiller (10 phr of LS). Further information concerning the preparation route of the nanocomposites, morphology detection and thermal characterization can be found elsewhere [11, 12].

Broadband dielectric measurements were performed, in the frequency range of 10^{-1} to 10^{6} Hz, by means of an Alpha-N Frequency Response Analyser, supplied by Novocontrol Technologies GmbH (Hundsangen, Germany). The BDS-1200, parallel-plate capacitor with two gold-plated electrodes supplied also by Novocontrol Technologies, was used as test cell. The dielectric cell was electrically shielded in nitrogen gas atmosphere and isothermal frequency scans were conducted for each of the examined specimens. Temperature was controlled by the Quattro system within ±0.1°C and varied between –100 and 50°C in steps of 5°C. The examined systems were: NR, PUR, PUR/NR, NR+10 phr LS, PUR+10 phr LS, PUR/NR+10 phr LS.

3. Results and discussion

Dielectric data can be analysed by means of different formalisms such as permittivity mode, modulus mode and ac conductivity mode. Electric modulus is defined as the inverse quantity of complex permittivity by the Equation (1):

$$M^* = \frac{1}{\varepsilon^*} = \frac{1}{\varepsilon' - j\varepsilon''} = \frac{\varepsilon'}{\varepsilon'^2 + \varepsilon''^2} + j\frac{\varepsilon''}{\varepsilon'^2 + \varepsilon''^2} = M' + jM'' \quad (1)$$

where ε', M' are the real and ε'', M'' the imaginary parts of dielectric permittivity and electric modulus, respectively. In the present study, experimental data were analysed via the electric modulus formalism. The interpretation of relaxation phenomena via the electric modulus formalism offers some advantages upon other treatments, since large variations in the permittivity and loss at low frequencies and high temperatures are minimized. Further, difficulties occurring from the electrode nature, the electrode-specimen contact and the injection of space charges and absorbed impurities can be neglected. Arguments concerning the resulting benefits

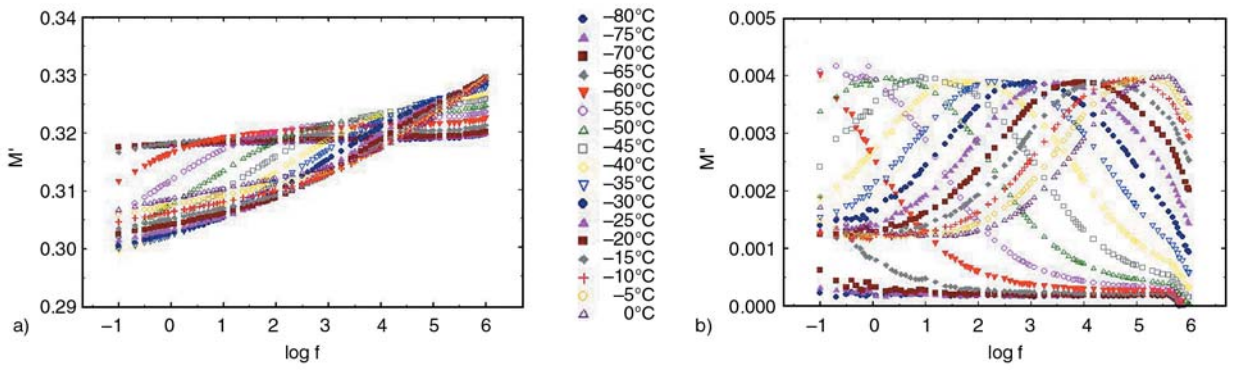

Figure 1. Real (a) and imaginary (b) part of electric modulus as a function of frequency for the NR specimen, in the low temperature range

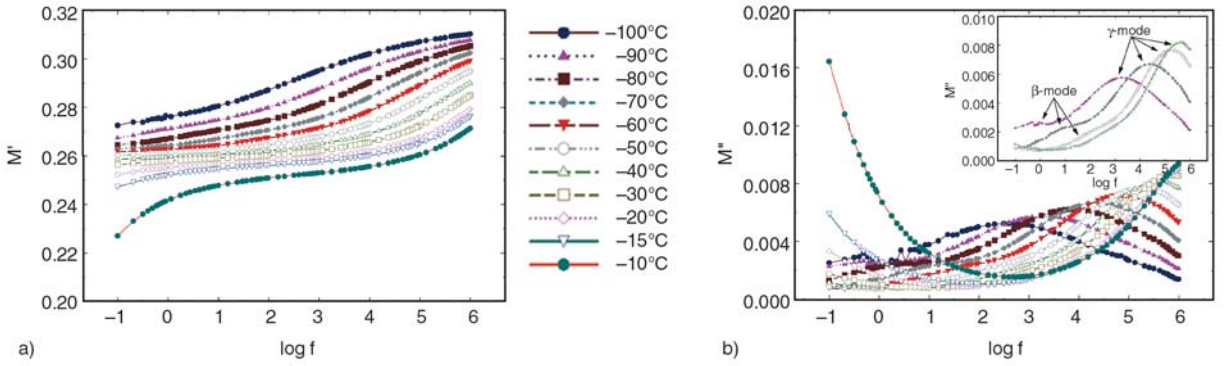

Figure 2. Real (a) and imaginary (b) part of electric modulus as a function of frequency for the PUR specimen, in the low temperature range. Inset presents isothermal plots at four selected temperatures

of the electric modulus presentation have been presented elsewhere [13–15].

The dielectric response of NR in the low temperature range is presented in Figure 1. NR is a non-polar polymer with glass transition temperature (T_g) very close to –64°C [12]. In the isothermal dielectric scans of NR (Figure 1) only one relaxation process is present. This process is recorded in the low temperature range, as expected, and is related to the glass/rubber transition of NR. Since no other processes are observed in the dielectric spectra of NR, its high temperature response is not presented here for the sake of brevity. Figures 2 and 3 depict the dielectric response of pure PUR in the low and high temperature ranges respectively. As it can be seen, PUR is a dielectrically active polymer exhibiting four distinct relaxation processes. All the recorded processes become evident via the step like transition from low to high values of the real part of electric modulus (M') and the corresponding peak of the imaginary part of electric modulus (M''). In some cases adjacent peaks are superimposed and the resulting dielectric spectrum consists of a 'shoulder-like' peak next to a well defined one. In the low temperature range, (Figure 2), two relatively fast processes occur, which are attributed, with descending frequency, to a 'crankshaft' type motion of the $(CH_2)_n$ sequence in the soft part of PUR (γ-mode) and to re-orientation of polar side groups of the main chain (β-mode). Inset in Figure 2b provides isothermal plots of M'' versus frequency at four selected temperatures. The relaxation peak of γ-mode is clearly formed at high frequencies, while β-mode is recorded in the low frequency edge. At higher temperatures, (Figure 3), two more mechanisms are clearly recorded. The one at higher frequencies, is ascribed to glass/rubber transition of PUR (α-mode), while the slow process is attributed to Interfacial Polarization (IP) or Maxwell-Wagner-Sillars (MWS) effect. Since electrode polarization is neglected in the electric modulus formalism [13–15] and the conductivity of all the tested specimens was low (Table 1) the slower process is unambiguously assigned to IP. IP appears in media exhibiting heterogeneity due to the accumulation of charges at the interfaces and the formation of large dipoles, which attempt to follow the alternation of the

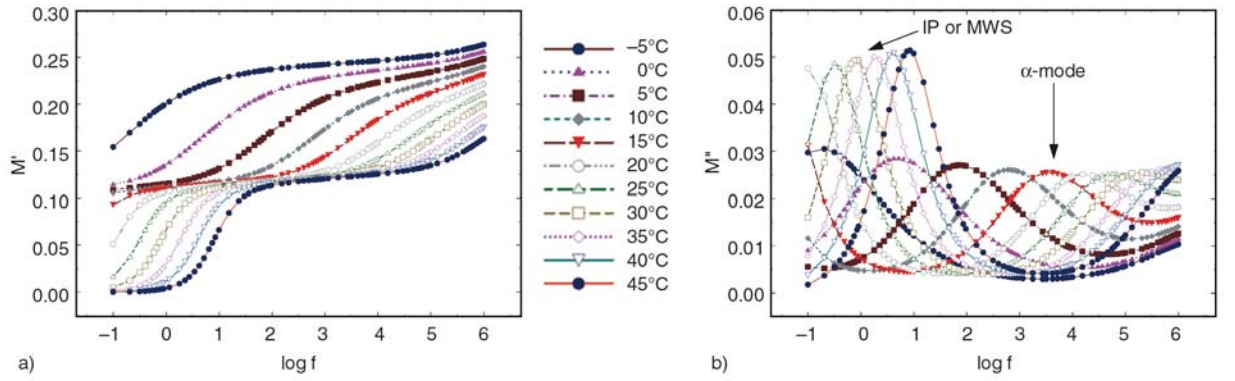

Figure 3. Real (a) and imaginary (b) part of electric modulus as a function of frequency for the PUR specimen, in the high temperature range

Table 1. Values of conductivity (σ)*, at three temperatures, for all the examined systems

Sample	σ [S·cm^{-1}]		
	–50°C	0°C	50°C
NR	$2.06\cdot10^{-15}$	$1.01\cdot10^{-15}$	$1.07\cdot10^{-13}$
PUR	$7.40\cdot10^{-16}$	$3.83\cdot10^{-14}$	$7.21\cdot10^{-11}$
PUR/NR	$8.89\cdot10^{-16}$	$1.44\cdot10^{-14}$	$6.79\cdot10^{-11}$
NR+10 phr LS	$2.99\cdot10^{-15}$	$6.82\cdot10^{-15}$	$3.62\cdot10^{-12}$
PUR+10 phr LS	$2.63\cdot10^{-14}$	$8.93\cdot10^{-13}$	$8.99\cdot10^{-11}$
PUR/NR+10 phr LS	$8.89\cdot10^{-16}$	$1.44\cdot10^{-14}$	$6.79\cdot10^{-11}$

*Conductivity values correspond to the lowest measured frequency of 10^{-1} Hz

applied electric field. IP is a slow relaxation process because of the inertia of the formed dipoles to acquire the orientation of the field. The repeat unit of PUR chain is composed by stiff, rigid blocks and soft rubbery blocks. In that sense IP arises from ionic polarization occurring at the interface of hard and soft regions as well as from variations of the morphology between amorphous and crystalline segments [16–18].

The dielectric spectra of the PUR/NR blend include contributions from both polymers, and thus in the low temperature range (Figure 4) the fast processes of local motions of small parts (β and γ-modes) of the PUR chain as well as the α-mode of NR are present. All three mechanisms occur, more or less, in the same frequency range and since the rate of peak shift with temperature varies from mode to mode, in many isothermal scans, peaks of different modes are superimposed, resulting in a complex curve. Furthermore, in the high temperature region, (Figure 5), two sets of peaks are obvious, corresponding to PUR's α-mode and IP respectively.

The real (M') and imaginary (M'') part of electric modulus for the NR+10 phr LS specimen, at low temperatures, is depicted in Figure 6. The dielectric profile of the LS reinforced NR resembles to that of the pure matrix. Besides glass/rubber transition of NR (α-mode) a second mechanism becomes apparent through the formation of broad or double peaks in the loss modulus (M'') index. The existence of an additional phase (viz. LS) introduces heterogeneity to the system leading to the appearance of IP. Previous work [11, 12] has shown that LS is less intercalated by NR than by PUR. Thus it is reasonable

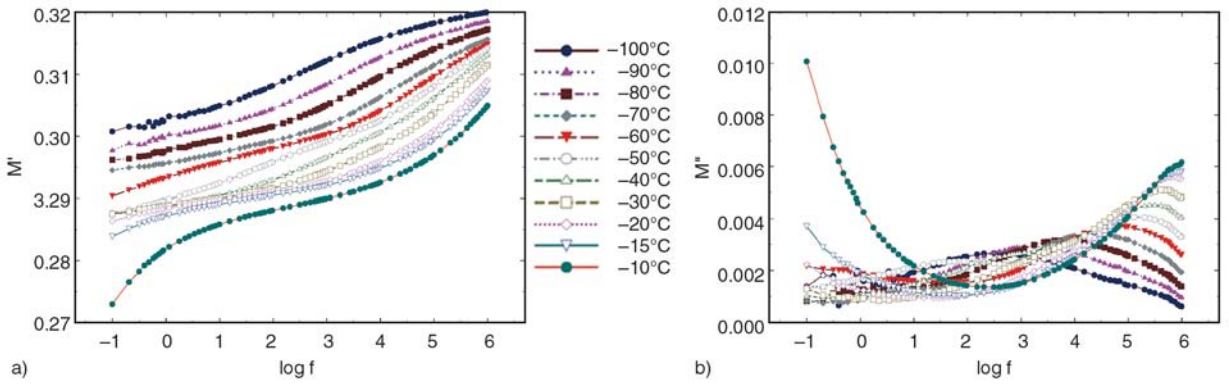

Figure 4. Real (a) and imaginary (b) part of electric modulus as a function of frequency for the PUR/NR specimen, in the low temperature range

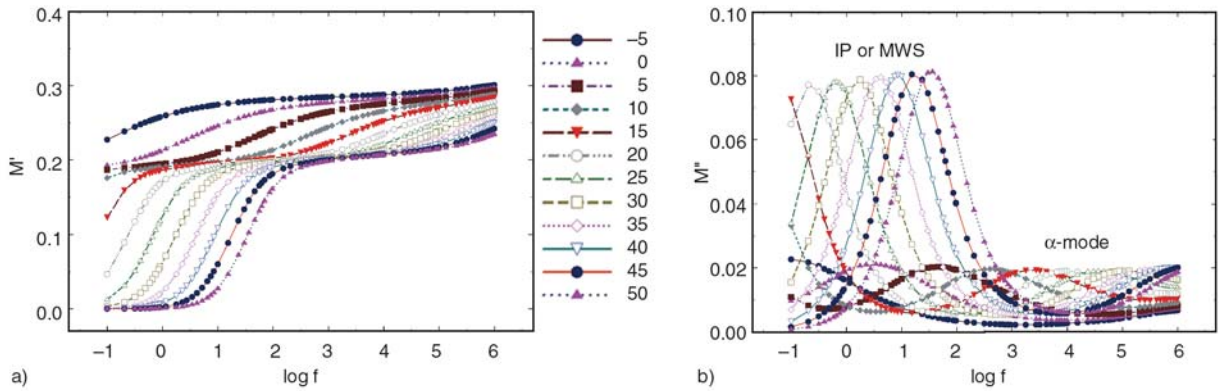

Figure 5. Real (a) and imaginary (b) part of electric modulus as a function of frequency for the PUR/NR specimen, in the high temperature range

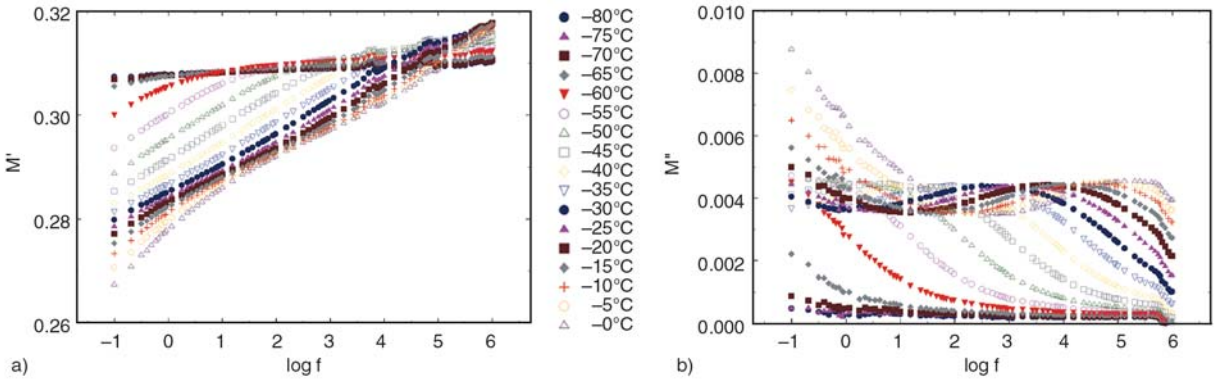

Figure 6. Real (a) and imaginary (b) part of electric modulus as a function of frequency for the NR+10 phr LS specimen, in the low temperature range

to suggest the co-existence of regions where LS remain immiscible with NR, leading to microphase separated composite structure, and regions where LS is intercalated by NR. These different morphologies affect both IP and α-mode. The interface between non-intercalated galleries of LS and NR gives rise to the formation of large dipoles, enhancing the electrical inertia of interfacial relaxation phenomenon, leading to slower motion or greater relaxation time. On the other hand, the interface between NR and intercalated LS results in the formation of relatively smaller dipoles allowing faster motion. Consequently, it is possible that the observed IP or MWS effect consists of two contributions, which differ in their relaxation rate. In addition, intercalation of polymer chains within the layers results in increased relaxation rate or lower glass transition temperature [12, 19, 20], since the isolated polymer molecules are not involved in cooperative molecular motions. The influence of all the above contributions is reflected in the broad and complex shape of the loss modulus (M'') curve with frequency (Figure 6b). For the same reasons, as in the case of pure NR, the high temperature dielectric response of NR+10 phr LS is omitted.

Figures 7 and 8 depict the dielectric behaviour of the PUR/NR+10 phr LS nanocomposite in the low and high temperature range respectively. Relaxations arising from IP as well as the contributions from both polymers (NR α-mode, PUR α, β and γ-modes) are recorded in the dielectric spectra. Finally, in Figures 9 and 10, the response of the PUR+10 phr LS nanocomposite is shown. The recorded relaxation mechanisms are, from the slower to the faster one, IP, glass/rubber transition (α-mode), and local motions of small parts of the polymer chain (β and γ-mode), as expected. In the low temperature region, (Figure 9), the existence of two processes becomes evident mostly via the transitions of the real part of electric modulus (M'), from low to high values, with frequency. The shape of the transitions, or more generally speaking, the variation of M' with frequency resembles that of PUR. In the plots of electric modulus loss index (M''), (Figure 9b), broad peaks are formed, with the location of their maxima shifted to lower frequen-

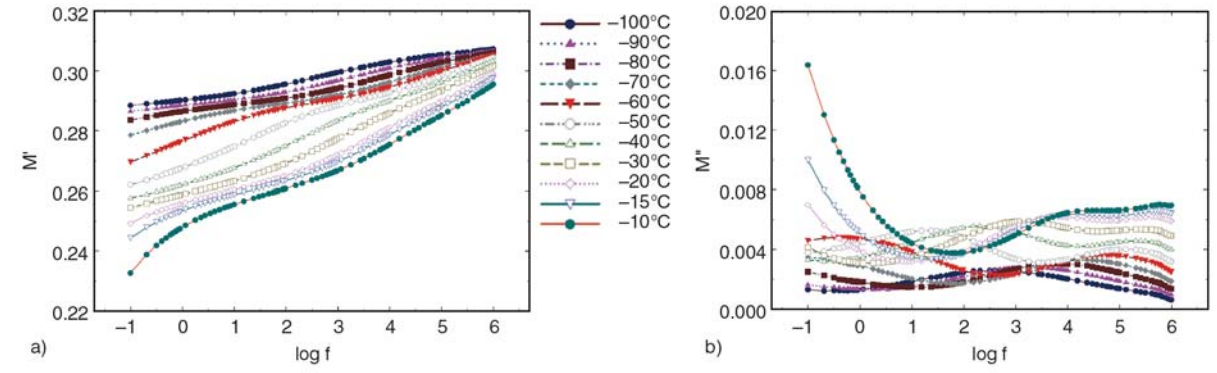

Figure 7. Real (a) and imaginary (b) part of electric modulus as a function of frequency for the PUR/NR+10 phr LS specimen, in the low temperature range

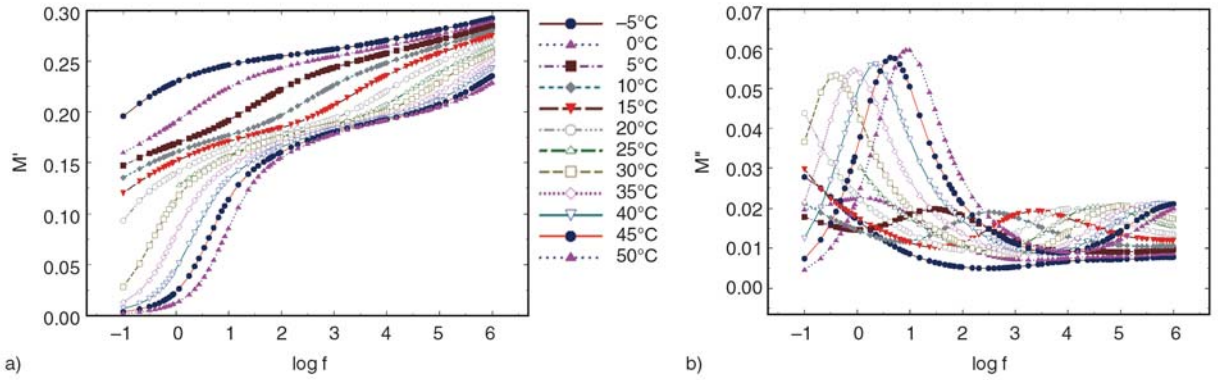

Figure 8. Real (a) and imaginary (b) part of electric modulus as a function of frequency for the PUR/NR+10 phr LS specimen, in the high temperature range

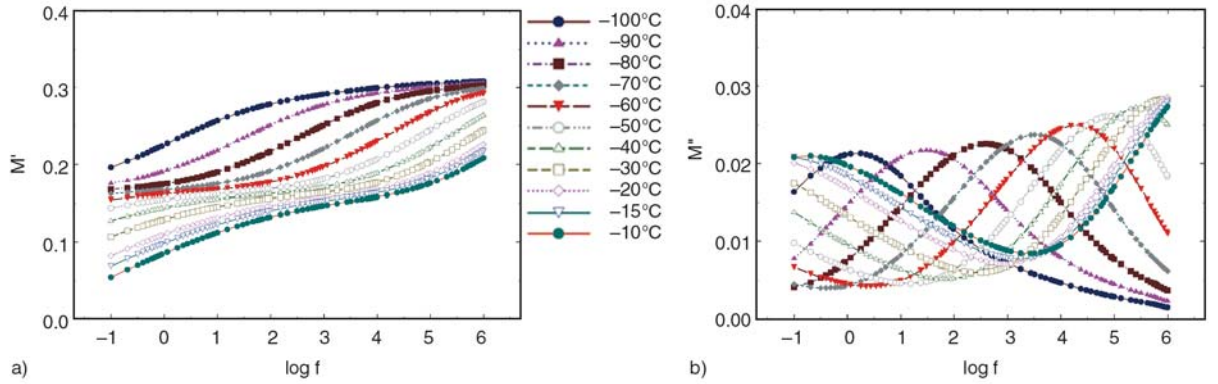

Figure 9. Real (a) and imaginary (b) part of electric modulus as a function of frequency for the PUR+10 phr LS specimen, in the low temperature range

cies compared to the corresponding peaks of PUR. In the case of pure PUR, γ-mode is more pronounced and β-mode is evident, at lower frequencies, as a shoulder-like peak. On the contrary, loss spectra of PUR+10 phr LS nanocomposite exhibit a clear peak in the same frequency range where β-mode is observed in PUR. This peak is superimposed with the peak of γ-mode on the high frequency edge. The inversion of the relative intensity between β and γ-modes could be an initial indication that the presence of LS restricts the evolution of γ-process. Since, γ-mode has been attributed to a 'crankshaft' type motion of the $(CH_2)_n$ sequence in the soft part of PUR chain, intercalated polymer molecules might not be able to follow the alternation of the field, repealing, up to a point, the motion of methyl groups. In the high temperature dielectric spectra of PUR+10 phr LS, IP and α-mode are detected. However, the behaviour differs in PUR+10 phr LS since this is the only case where the amplitude of the recorded IP peak is lower than the corresponding of glass/rubber relaxation (α-mode). Interfacial relaxation phenomena are prominent in the low frequency range and relatively high temperatures, resulting in high values of both real and imaginary part of dielectric permittivity [14, 15, 21]. Further increase of the intensity of interfacial effects results in even higher values of (ε′) and (ε″). On the other hand, in the electric modulus presentation, the increase of intensity of IP (MWS effect) is demonstrated by reduced values of M' and M''. Thus it can be concluded that the lower values of the modulus loss index (M'') is a strong indication for the existence of pronounced interfacial phenomena in the PUR+10 phr LS system (Figure 10b). Additionally, the broadness of the corresponding peak should be related to interactions between the constituents of the nanocomposite. Previous studies [11, 12] upon the morphology of PUR+10 phr LS have shown the existence of two intercalated populations with different interlayer distances, namely 1.23 and 1.73 nm. Moreover, the presence of isolated silicate layers due to partial exfoliation cannot be excluded. Under this point of view, interfaces with varying geometrical characteristics contribute to interfacial relaxation phe-

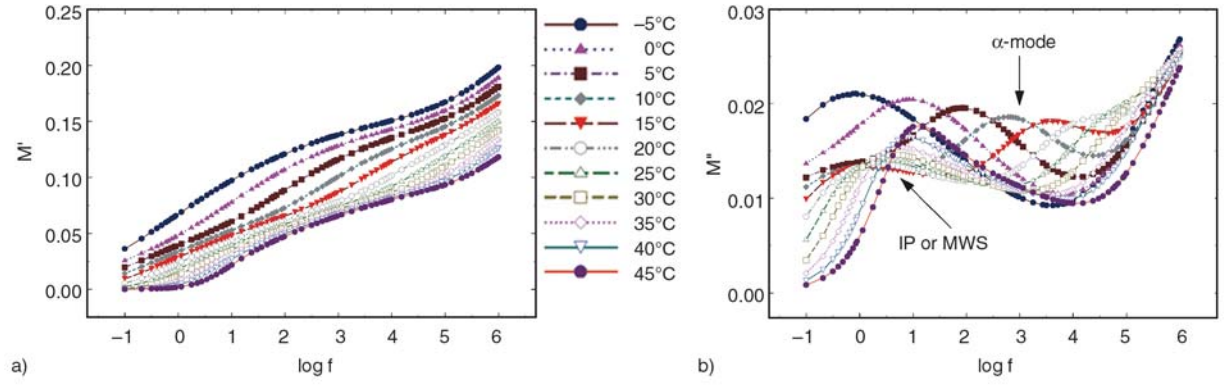

Figure 10. Real (a) and imaginary (b) part of electric modulus as a function of frequency for the PUR+10 phr LS specimen, in the high temperature range

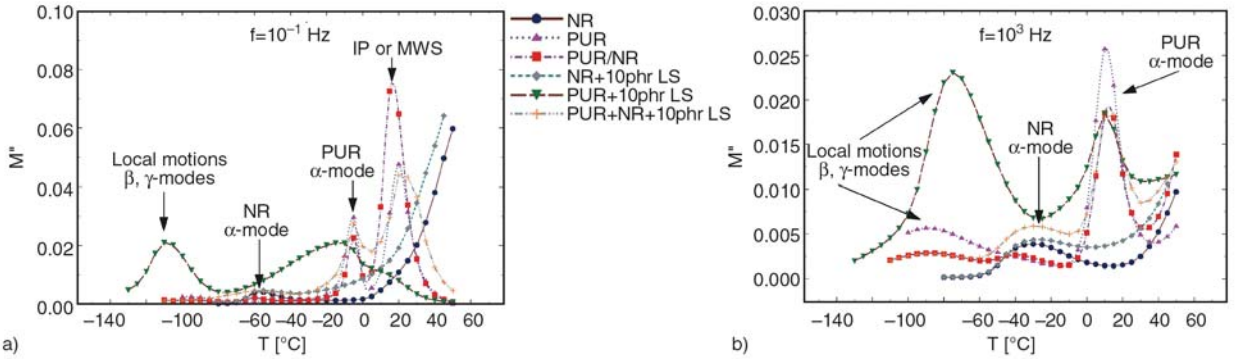

Figure 11. Imaginary part of electric modulus as a function of temperature for all the examined specimens at (a) $f = 10^{-1}$ Hz and (b) $f = 10^{3}$ Hz

nomena with different dynamics or relaxation times. Superposition of all interfacial effects forms the recorded broad peak.

For reasons of comparison, isochronal plots of all the examined systems are presented in Figure 11. The occurring relaxation mechanisms are indicated by arrows, and a direct comparison, supporting the above discussion, can be easily conducted.

It is well known, from dielectric theory, that the frequency-temperature superposition shifts the loss peak position of relaxation processes to higher frequencies with increasing temperature. The temperature dependence of the electric modulus loss (M'') maxima loci for both IP and α-mode, is depicted in Figure 12, for all the examined systems. The temperature dependence of peak shift is a measure of the relaxation rate of the specific process. IP follows the Arrhenius type temperature dependence, which is expressed by the Equation (2):

$$f = f_0 \exp\left(-\frac{E_A}{k_B T}\right) \tag{2}$$

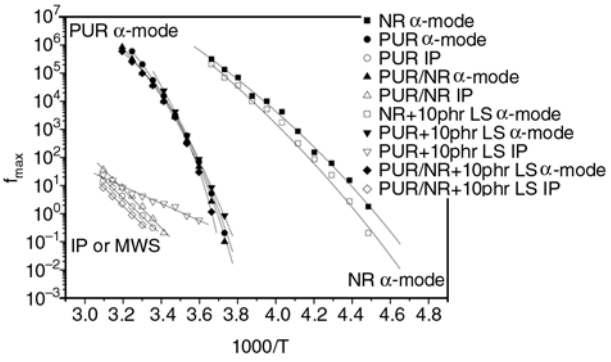

Figure 12. Loss peak position as a function of inverse temperature of the slow processes (IP and α-mode), for all the examined specimens

where E_A is the activation energy, f_0 pre-exponential constant and k_B the Boltzmann constant. In contrary, the temperature dependence of α-mode deviates from Equation (2) following the Vogel-Fulcher-Tamann (VTF) equation, which considers that relaxation rate increases rapidly at lower temperatures because of the reduction of the free volume.

VTF equation is given by (3):

Table 2. Values of activation energy, calculated via Equation (2), for the IP mode and fitting parameters of Equation (3) for α-mode

Sample	A [K^{-1}]	T_0 [K]	E_A [eV]
NR	25.7	128	–
PUR	8.3	215	1.29
PUR/NR	5.8	225	1.37
NR+10 phr LS	35.0	120	–
PUR+10 phr LS	33.0	165	0.60
PUR/NR+10 phr LS	2.4	246	1.29

$$f = f_0 \exp\left(-\frac{AT_0}{T - T_0}\right) \tag{3}$$

where f_0 is a pre-exponential factor, A a constant (being a measure of the activation energy), and T_0 Vogel temperature or ideal glass transition temperature. The values of activation energy for IP-mode, calculated via linear regression, as well as all fitted parameters of Equation (3), for each of the tested systems, are listed in Table 2. Going back to Figure 12 three sets of curves can be distinguished. The first one, recorded at the higher temperatures, corresponds to IP. As it can be seen, all curves display proximity with the only exception of PUR+10 phr LS nanocomposite. The slope of this curve deviates remarkably leading to a significantly lower value of activation energy (Table 2) implying an easier activated relaxation process. The second set of curves corresponds to α-mode of PUR and is recorded at intermediate temperatures. Finally, the third set recorded at low temperatures, corresponds to α-mode of NR.

4. Conclusions

Based on the experimental data from dielectric spectroscopy and the analysis carried out the following conclusions can be drawn. NR is a material of low dielectric permittivity and loss, and its α-mode is recorded in the low temperature range due to its low glass transition temperature. PUR is a dielectrically active polymer exhibiting four distinct relaxation processes, namely IP, glass/rubber transition (α-mode), β- and γ-relaxation modes resulting from the motion of polar side groups and local motions of small chain segments (motions of the $(CH_2)_n$ sequences). The same processes can be detected in all systems containing PUR. Interfacial Polarization is present in all nanocomposites and is detected in the low frequency range and relatively high temperatures, being the slowest recorded process. Finally, pronounced interfacial relaxation phenomena, occurring in the PUR+10 phr LS spectra, are attributed to the existence of different intercalated populations and to possible partial exfoliation of LS.

Acknowledgements

This work was supported by the PPP IKYDA 2005 program between DAAD and IKY (Greek State Scholarships Foundation).

References

[1] Thostenson E. T., Ren Z., Chou T-W.: Advances in the science and technology of carbon nanotubes and their composites: A review. Composites Science and Technology, **61**, 1899–1912 (2001).

[2] Karger-Kocsis J., Wu C-M.: Thermoset rubber/layered silicate nanocomposites. Status and future trends. Polymer Engineering and Science, **44**, 1083–1093 (2004).

[3] Jordan J., Jacob K. I., Tannenbaum R., Sharaf M. A., Jasiuk I.: Experimental trends in polymer nanocomposites: A review. Materials Science and Engineering, Part A: Structural Materials, **393**, 1–11 (2005).

[4] Auad M. L., Nutt S. R., Pettarin V., Frontini P. M.: Synthesis and properties of epoxy-phenolic clay nanocomposites. Express Polymer Letters, **1**, 629–639 (2007).

[5] Tanaka T., Montari G. C., Mülhaupt R.: Polymer nanocomposites as dielectrics and electrical insulation-perspectives for processing technologies, materials characterization and future applications. IEEE Transactions on Dielectrics and Electrical Insulation, **11**, 763–783 (2004).

[6] Montari G. C., Fabiani D., Palmieri F., Kaempfer D., Thomann R., Mülhaupt R.: Modification of electrical properties and performance of EVA and PP insulation through nanostructure by organophilic silicates. IEEE Transactions on Dielectrics and Electrical Insulation, **11**, 754–762 (2004).

[7] Pegoretti A., Dorigato A., Penati A.: Tensile mechanical response of polyethylene-clay nanocomposites. Express Polymer Letters, **1**, 123–131 (2007).

[8] Abacha N., Kubouchi M., Tsuda K., Sakai T.: Performance of epoxy-nanocomposite under corrosive environment. Express Polymer Letters, **1**, 364–369 (2007).

[9] Fréchette M. F., Trudeau M., Alamdari H. D., Boily S.: Introductory remarks on nanodielectrics. in 'IEEE Conference on Electrical Insulation and Dielectric Phenomena (CEIDP). Kitchener, Canada', 92–99 (2001).

[10] Kremer F., Schönhals A.: Broadband dielectric measurement techniques (10^{-6} Hz to 10^{12} Hz). in 'Broadband dielectric spectroscopy' (ed(s).: Kremer F., Schönhals A.) Springer, Berlin, 35–64 (2003).

[11] Varghese S., Gatos K. G., Apostolov A. A., Karger-Kocsis J.: Morphology and mechanical properties of layered silicate reinforced natural and polyurethane rubber blends produced by latex compounding. Journal of Applied Polymer Science, **92**, 543–551 (2004).

[12] Psarras G. C., Gatos K. G., Karger-Kocsis J.: Dielectric properties of layered silicate reinforced natural and polyurethane rubber nanocomposites. Journal of Applied Polymer Science, **106**, 1405–1411 (2007).

[13] Tsangaris G. M., Psarras G. C., Kouloumbi N.: Electric modulus and interfacial polarization in composite polymeric systems. Journal of Materials Science, **33**, 2027–2037 (1998).

[14] Psarras G. C., Manolakaki E., Tsangaris G. M.: Electrical relaxations in polymeric particulate composites of epoxy resin and metal particles. Composites, Part A: Applied Science and Manufacturing, **33**, 375–384 (2002).

[15] Psarras G. C., Manolakaki E., Tsangaris G. M.: Dielectric dispersion and ac conductivity in-iron particles loaded-polymer composites. Composites, Part A: Applied Science and Manufacturing, **34**, 1187–1198 (2003).

[16] Pissis P., Kanapitsas A., Savelyev Y. V., Akhranovich E. R., Privalko E. G.: Influence of chain extenders and chain end groups on properties of segmented polyurethanes. II. Dielectric study. Polymer, **39**, 3431–3435 (1998).

[17] Korzhenko A., Tabellout M., Emery J. R.: Influence of a metal-polymer interfacial interaction on dielectric relaxation properties of polyurethane. Polymer, **40**, 7187–7195 (1999).

[18] Gatos K. G., Martínez Alcázar J. G., Psarras G. C., Thomann R., Karger-Kocsis J.: Polyurethane latex/water dispersible boehmite alumina nanocomposites: Thermal, mechanical and dielectrical properties. Composites Science and Technology, **67**, 157–167 (2007).

[19] Elmahdy M. M., Chrissopoulou K., Afratis A., Floudas G., Anastasiadis S. H.: Effect of confinement on polymer segmental motion and ion mobility in PEO/Layered silicate nanocomposites. Macromolecules, **39**, 5170–5173 (2006).

[20] Anastasiadis S. H., Karatasos K., Vlachos G., Manias E., Giannelis E. P.: Nanoscopic-confinement effects on local dynamics. Physical Review Letters, **84**, 915–918 (2000).

[21] Tsangaris G. M., Psarras G. C.: The dielectric response of a polymeric three-component composite. Journal of Materials Science, **34**, 2151–2157 (1999).